EXAFS Measurement of Iron bcc-to-hcp Phase Transformation in Nanosecond-Laser Shocks

B. Yaakobi, T. R. Boehly, D. D. Meyerhofer, and T. J. B. Collins
Laboratory for Laser Energetics, University of Rochester, 250 East River Road, Rochester, New York 14623, USA

B. A. Remington, P. G. Allen, S. M. Pollaine, H. E. Lorenzana, and J. H. Eggert
Lawrence Livermore National Laboratory, Livermore, California 94550, USA
(Received 26 April 2005; published 9 August 2005)

Extended x-ray absorption fine structure (EXAFS) measurements have demonstrated the phase transformation from body-centered-cubic (bcc) to hexagonal-close-packed (hcp) iron due to nanosecond, laser-generated shocks. The EXAFS spectra are also used to determine the compression and temperature in the shocked iron, which are consistent with hydrodynamic simulations and with the compression inferred from velocity interferometry. This is a direct, atomic-level, and *in situ* proof of shock-induced transformation in iron, as opposed to the previous indirect proof based on shock-wave splitting.

DOI: 10.1103/PhysRevLett.95.075501 PACS numbers: 64.70.Kb, 61.10.Ht, 61.80.Ba, 62.50.+p

The dynamics of material response to shock loading has been extensively studied in the past [1]. The goal of those studies was to understand the shock-induced deformation and structural changes at the microscopic level. Laser-generated shocks have been recently employed [2] to broaden these studies to higher pressures ($\sim$100 GPa) and strain rates ($\sim 10^7$ to 10^8 s^{-1}). The use of *in situ* extended x-ray absorption fine structure (EXAFS) for characterizing nanosecond-laser-shocked vanadium and titanium has been recently demonstrated [3]. Additionally, the observed fast decay of the EXAFS modulations in titanium shocked to $\sim$40 GPa was shown [3] to be due to the α-Ti to ω-Ti phase transformation. We show here that EXAFS can likewise be used to demonstrate the bcc-to-hcp phase transformation in iron. This same nanosecond, laser-induced transformation was also demonstrated using *in situ* x-ray diffraction, as described in the following Letter [4]. Initially, Bancroft *et al.* [5] showed that the multiple fronts propagating within a shocked iron indicated a phase transformation at about 13 GPa. Subsequently, Jamieson and Lawson have shown [6] by diffraction in a diamond anvil cell that a bcc-to-hcp phase transformation, indeed, occurs at about 13 GPa. The historical importance of this transition is that it was observed first under shocked rather than static compression. It also established the reliability of shocks for obtaining pressure-compression relations. The transformation has been extensively studied in gas-gun shock experiments [7,8] using the velocity history of the back surface of the target, where a long ($\gg$10 ns) characteristic time for the transformation was deduced. This contrasts with the subnanosecond time derived in the present experiment. The longer times deduced from velocity measurements [7] have been explained [8] in terms of the pressure dependence of the characteristic time. Using Fig. 5 of Ref. [8] we can estimate a characteristic time for iron at a pressure of 35 GPa of $\sim$5 ns. Much shorter times have been inferred from the residual microstructure that is quenched after the passage of nanosecond and even subnanosecond shocks [9]. The observation here of the transformation in nanosecond-laser shocks confirms the latter finding. Unlike the evidence [9] derived from the examination of residual microstructure after the experiment, the measurements here are *in situ*.

The EXAFS spectrum of iron is markedly different in the bcc (or α-Fe) phase as compared with the hcp (or ε-Fe) phase [10]; this provides a signature for identifying the transformation in laser-shock experiments. Transient phase-transformation experiments require methods for characterizing the crystal conditions (e.g., the pressure) during the transformation, in order to substantiate the occurrence of the transformation. In static compression experiments the temperature and pressure are independently controlled and measured. Here we show that the temperature and compression (and, hence, the pressure) can be deduced from the EXAFS record itself, in addition to providing evidence of the phase transformation.

K-edge EXAFS measurements were performed on iron shocked to $\sim$35 GPa with a 3 ns laser pulse, provided by 3 of the 60 beams of the OMEGA laser [11]. The radiation source for the EXAFS measurement was obtained by imploding a spherical target using the remaining 57 OMEGA beams. In a previous paper [12] we showed that a CH shell imploded by a multibeam laser system emits intense and spectrally smooth radiation, lasting $\sim$120 ps, and suitable for EXAFS measurements on nanosecond time scales.

The experimental configuration in this work was identical to that used in our previous EXAFS experiments [3]. Two cross-calibrated, flat-crystal spectrometers were used for measuring the incident and transmitted spectra on a single laser shot. The planar target consisted of 8 μm thick polycrystalline iron (purity of 99.85%), coated on both sides with 17 μm thick CH; thus, the iron layer is directly affected by the shock but not by the laser absorption and heating. The delay time of the three-stacked beams with respect to the remaining beams was adjusted so that peak implosion (and emission) of the spherical

target occurred just when the shock wave exited the metal layer.

The expected shock strength and the properties of the shocked iron were determined using one-dimensional (1D) simulations with the hydrodynamic code LASNEX [13]. The tabular equation of state incorporated into the code includes the α-Fe to ε-Fe phase transformation. Figure 1 shows the computed profiles just as the shock exits the iron layer. The volume-averaged values are pressure 36 GPa, temperature 645 K, and compression 1.2 (or 20%). The measured spectra were analyzed with the FEFF8 *ab initio* EXAFS software package [14]. The basic theory of EXAFS [15] yields an expression for the relative absorption $\chi(k) = \mu(k)/\mu_0(k) - 1$, where $\mu(k)$ is the absorption coefficient and $\mu_0(k)$ is the absorption of the isolated atom. The wave number k of the ejected photoelectron is given by the de Broglie relation $\hbar^2 k^2/2m = E - E_K$, where E is the absorbed photon energy and E_K is the energy of the K edge. FEFF8 uses the scattering potential to calculate the amplitude and phase shift of the photoelectron waves scattered from several shells of neighboring atoms including multiple-scattering paths. The main fitting parameters are the nearest-neighbor distance R and the vibration amplitude σ^2 appearing in the Debye-Waller term [15]. R yields the density or compression; σ^2 as a function of temperature was calculated using the Debye model [16] for the phonon density of states, including correlation, and it also depends on the density through the Debye temperature. The density dependence of the Debye temperature for Fe-ε was taken from published measurements [17]. The results can be approximated by $\sigma^2(\text{Å}^2) = 0.001 + 2 \times 10^{-5} T(\text{K})/C^{3.58}$, where $C = (\rho/\rho_0)$ is the compression ratio. Using this dependence and the result for σ^2 from FEFF8 fitting, the temperature can be derived.

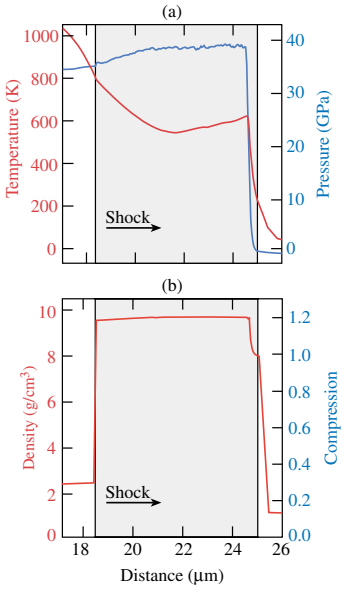

FIG. 1 (color). Profiles of (a) target pressure and temperature and (b) density calculated by LASNEX (the iron layer, enclosed within CH layers, is highlighted). The laser propagates towards the right.

In order to assess the reliability of our Fe EXAFS measurements, we obtained the EXAFS spectrum for unshocked iron, using the configuration described above but without firing the shock-launching beams. Figure 2 shows a comparison between the resulting absorption and a standard iron absorption spectrum measured at the Stanford Synchrotron Radiation Laboratory. The agreement is seen to be good.

EXAFS provides a very distinct, qualitative signature for the bcc-to-hcp phase transformation in iron [10]. This is demonstrated by Fig. 3, showing (a) the EXAFS spectrum for the two phases calculated by the FEFF8 code and (b) the EXAFS spectrum measured on OMEGA for unshocked and shocked iron. Anticipating the fitting results described below, a compression of 20% (with respect to the initial bcc density) and a temperature of 700 K were assumed in Fig. 3(a) for the hcp phase. The bcc calculation is for room-temperature and ambient-pressure conditions. The main signature of the phase transformation is seen to be the disappearance of the peak marked W. When the calculations for the bcc phase are repeated for a wide range of compressions, the feature W remains intact. Thus, its disappearance can only be due to the phase transformation, not due to the shock compression (we later show that this is true even in the case of 1D compression). The W feature arises from a coincidence in peaks of waves scattered from the third and fourth neighboring shells in the bcc crystal. No such coincidence occurs in the hcp crystal. The effect of compression on the EXAFS spectrum is to increase the period of oscillation (in k space) and that of the heating is to cause the oscillations to decay faster with increasing k; both are evident in Fig. 3(a).

The experimental results shown in Fig. 3(b) mirror the changes seen in Fig. 3(a). Compression and heating are evident, and the disappearance of the W feature indicates a bcc-to-hcp phase transformation. The complete disappearance of that feature indicates that the transformation is complete, hence that its time constant must be shorter than $\sim$1 nsec. Additionally, the predicted enhancement in the peak at about $k \sim 3\,\text{Å}^{-1}$ is also observed in Fig. 3(b). These results were consistently observed on repeated ex-

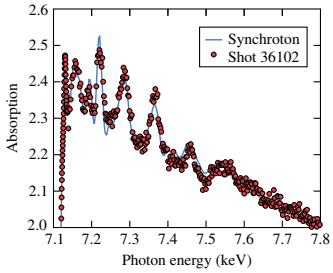

FIG. 2 (color). Comparison of the measured absorption of unshocked iron on OMEGA and a standard iron EXAFS measured at the Stanford Synchrotron Radiation Laboratory.

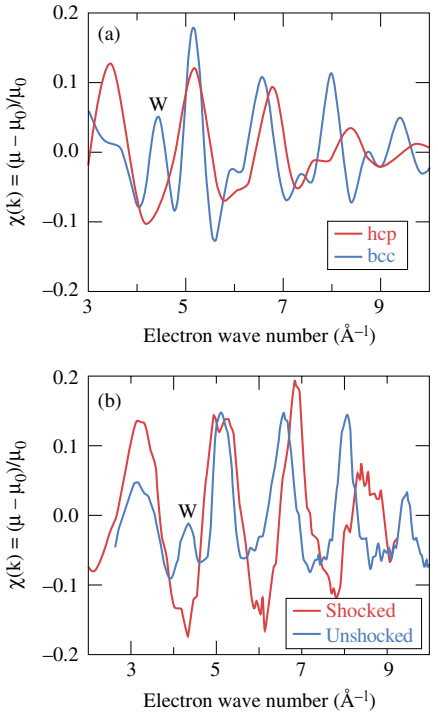

FIG. 3 (color). (a) FEFF8 calculation of the EXAFS spectrum for unshocked α-Fe (bcc) and ε-Fe (hcp), compressed by 20% with respect to the initial bcc iron. (b) Experimental results for unshocked and shocked iron. The disappearance of the peak marked W is a signature of phase transformation.

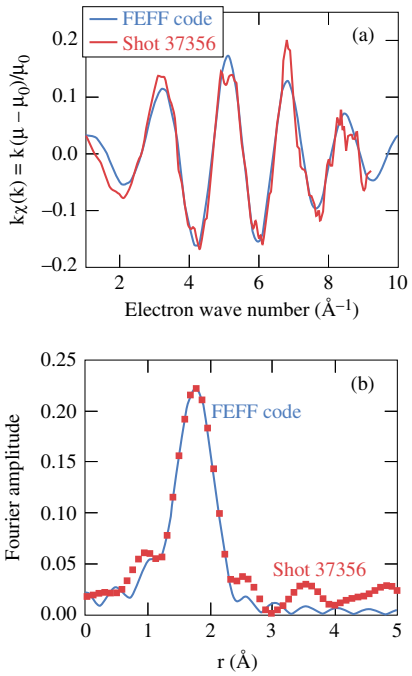

FIG. 4 (color). FEFF8 code fitting to the experimental results, assuming the hcp phase: (a) in the k space, (b) in the r space.

periments under the same conditions. These conclusions are borne out by the more precise fitting analysis below.

We now turn to FEFF fitting to the experimental EXAFS spectra. As Fig. 3 shows, we cannot fit the data with bcc EXAFS spectra; the two are qualitatively different. On the other hand, hcp calculated EXAFS agrees well with the experimental EXAFS data. Figure 4 shows the best fits, in wave number (k) space and in distance (r) space. The fit in r space (where the spectrum shows the spatial charge distribution around the absorbing atom) is obtained by Fourier transforming the experimental as well as the theoretical curves in k space [15]. The dimensions a and c of the hcp unit cell are known as a function of hydrostatic compression [18] (for all compressions $c/a \sim 1.6$) and thus the bond length (or nearest-neighbor distance) R is simply related to the compression under such conditions (we discuss the implications of finite shear strength below). Note that the value of R corresponding to the best fit is larger than the position of the peak in Fig. 4(b) because of the phase factors in the wave scattering. The fitting yields $R = (2.39 \pm 0.0133)$ Å, which corresponds to a compression of 1.22 ± 0.023. This value agrees well with the average compression of 1.2 predicted by LASNEX [see Fig. 1(b)]. Turning now to the estimate of temperature, the FEFF best fit to the data [Fig. 4(a)] corresponds to $\sigma^2 = 0.0078 \pm 0.0030$ Å^2. This value of σ^2 corresponds to a temperature of 670 ± 170 K, thus agreeing well with the average temperature 645 K predicted by LASNEX [Fig. 1(a)]. Using the equation of state of iron and the measured temperature and compression values leads to an estimate of the pressure as $\sim$35 GPa. LASNEX uses the equation of state of iron, which includes the α to ε phase transformation (but not its kinetics). These values also agree with the equation of state calculated for the Hugoniot of iron [19]. The deduced pressure is well above the pressure of slower shocks in iron where a bcc-to-hcp phase transformation takes place [18]. Also, the derived values of pressure and temperature correspond to a point on the phase diagram of iron [5] that is well within the Fe-ε (hcp) region.

Velocity interferometric (VISAR) measurements [20] were performed on iron targets identical to those used for the EXAFS measurements, except that the CH coating was placed only on the side facing the laser. In this way the velocity of the iron-free back surface could be measured. From the surface velocity the particle velocity could be determined by dividing by 2. This relationship has been shown [21] to hold for iron shocked to pressures of up to $\sim$150 GPa. Because of the relatively high pressure and the small foil thickness in this experiment, the velocity waves [7,8] indicative of transition to plastic flow and of a phase transformation were not resolved; thus the VISAR results cannot confirm either transition. However, the deduced particle velocity can be used with the known Hugoniot curve of iron to determine the compression. For the measured rear-surface velocity of 1.5×10^5 cm/s the resulting compression is $C = 1.17$, in agreement with the values predicted by LASNEX and with the values measured by EXAFS (using the FEFF8-code fitting).

The analysis above has assumed that the compression of the hcp crystal, but not necessarily that of the bcc crystal, is hydrostatic. The dynamical yield stress in polycrystalline iron has been found to be lower than 1 GPa [22], using mm-scale specimen thicknesses and strain rates of order 10^5 s^{-1}. Because the dynamic yield stress in iron increases with strain rate as well as with decreasing specimen thickness [22], we cannot assume plastic compression of the bcc crystal prior to the phase transformation; in thin iron samples the Hugoniot elastic limit can be higher than the pressure for phase transformation [23]. However, the transformation involves atomic motions in various mutually perpendicular directions in the bcc phase [10,24], thus also in a direction perpendicular to the shock direction; this should lead to relaxation of the shear stress. In the hcp phase the first shell of nearest neighbors, whose distance is given by the unit-cell parameter a, has a major contribution to the EXAFS spectrum; thus, the analysis determines primarily a, whereas the unit-cell parameter c is primarily needed for the calculation of volume compression. Therefore, values of c/a somewhat different from the static values used here cannot be excluded. However, such values would still imply a compression consistent within experimental error with the compression obtained by VISAR measurements and by hydrodynamic simulations.

Since the possibility of elastic compression of the bcc crystal cannot be discounted, the following question arises: Can the observed EXAFS be explained by a 1D compression of the bcc crystal *with no* phase transformation? In other words, would the W peak disappear due to one-dimensional compression where no phase transformation takes place. To answer this question, we calculated the EXAFS spectrum assuming that atomic coordinates in the bcc crystal are reduced only in the shock direction. Since in a polycrystalline sample the grains are oriented randomly, the angles between the crystal axes and the shock direction assumes all possible values. Therefore, the result was averaged over all these angles. For simplicity, only single scattering from the first four nearest-neighbor shells was considered, using the scattering amplitudes and phase shifts from the tables of Teo and Lee [25]. The 1D compression value was varied to match the experimental frequency of modulation, resulting in 12% compression (in slower shocks the transformation starts to occur at a compression of ~6%). Since the W feature in these calculations has not disappeared upon 1D compression (nor has the first peak increased in intensity), the measured EXAFS spectra cannot be explained as resulting from a 1D compression without a phase transformation. Thus, only the analysis assuming the hcp phase agrees with the measurement.

This work was supported by the U.S. Department of Energy Office of Inertial Confinement Fusion under Cooperative Agreement No. DE-FC03-92SF1931,460, the University of Rochester, and the New York State Energy Research and Development Authority. The support of DOE does not constitute an endorsement by DOE of the views expressed in this Letter. Portions of this research were carried out at the Stanford Synchrotron Radiation Laboratory, a national user facility operated by Stanford University on behalf of the U.S. Department of Energy, Office of Basic Energy Sciences. Portions of this work were performed under the auspices of the U.S. Department of Energy by the University of California, Lawrence Livermore National Laboratory (LLNL) under Contract No. W-7405-Eng-48. Additional support was provided by LDRD Project No. 04-ERD-071 at LLNL.

[1] J. E. Dorn and S. Rajnak, Trans. TMS-AIME **230**, 1052 (1964); U. F. Kocks, A. S. Argon, and M. F. Ashby, *Thermodynamics and Kinetics of Slip* (Pergamon, New York, 1975); M. A. Myers and L. E. Murr, *Shock Waves and High-Strain-Rate Phenomena in Metals: Concepts and Applications* (Plenum, New York, 1981).
[2] B. A. Remington *et al.*, Metall. Mater. Trans. A **35**, 2587 (2004).
[3] B. Yaakobi *et al.*, Phys. Rev. Lett. **92**, 095504 (2004); B. Yaakobi *et al.*, Phys. Plasmas **11**, 2688 (2004).
[4] D. H. Kalanter *et al.*, Phys. Rev. Lett. **95**, 075502 (2005).
[5] D. Bancroft, E. L. Peterson, and S. Minshall, J. Appl. Phys. **27**, 291 (1956).
[6] J. C. Jamieson and A. W. Lawson, J. Appl. Phys. **33**, 776 (1962).
[7] L. M. Barker and R. E. Hollenbach, J. Appl. Phys. **45**, 4872 (1974).
[8] J. C. Boettger and D. C. Wallace, Phys. Rev. B **55**, 2840 (1997).
[9] C. S. Smith, Trans. TMS-AIME **212**, 574 (1958); T. Sano, H. Mori, E. Ohmura, and I. Miyamoto, Appl. Phys. Lett. **83**, 3498 (2003).
[10] F. M. Wang and R. Ingalls, Phys. Rev. B **57**, 5647 (1998).
[11] T. R. Boehly *et al.*, Rev. Sci. Instrum. **66**, 508 (1995).
[12] B. Yaakobi *et al.*, J. Opt. Soc. Am. B **20**, 238 (2003).
[13] G. B. Zimmerman and W. L. Kruer, Comments Plasma Phys. Control. Fusion **2**, 51 (1975).
[14] J. J. Rehr, R. C. Albers, and S. I. Zabinsky, Phys. Rev. Lett. **69**, 3397 (1992).
[15] P. A. Lee *et al.*, Rev. Mod. Phys. **53**, 769 (1981).
[16] E. Sevillano, H. Meuth, and J. J. Rehr, Phys. Rev. B **20**, 4908 (1979).
[17] L. S. Dubrovinsky *et al.*, Am. Mineral. **85**, 386 (2000).
[18] A. P. Jephcoat, H. K. Mao, and P. M. Bell, J. Geophys. Res. **91**, 4677 (1986).
[19] R. G. McQueen *et al.*, in *High-Velocity Impact Phenomena*, edited by R. Kinslow (Academic, New York, 1970), Chap VII and Appendix E.
[20] P. M. Celliers *et al.*, Appl. Phys. Lett. **73**, 1320 (1998).
[21] L. V. Al'tshuler *et al.*, Sov. Phys. JETP **11**, 573 (1960).
[22] R. W. Rohde, Acta Metall. **17**, 353 (1969).
[23] G. E. Duvall, *Shock Waves and High-Strain-Rate Phenomena in Metals*, edited by M. A. Meyers and L. E. Murr (Plenum Press, New York, 1981), Chap. 40.
[24] V. P. Dmitriev, Yu. M. Gufan, and P. Toledano, Phys. Rev. B **44**, 7248 (1991).
[25] B.-K. Teo and P. A. Lee, J. Am. Chem. Soc. **101**, 2815 (1979).